1989

NASA/ASEE SUMMER FACULTY FELLOWSHIP PROGRAM

MARSHALL SPACE FLIGHT CENTER
THE UNIVERSITY OF ALABAMA IN HUNTSVILLE

MONTE CARLO MODELS AND ANALYSIS OF GALACTIC DISK GAMMA-RAY BURST DISTRIBUTIONS

Prepared by:	Jon Hakkila
Academic Rank:	Assistant Professor
University and Department:	Mankato State University Department of Mathematics, Astronomy, and Statistics
NASA/MSFC:	
Laboratory:	Space Science
Division:	Astrophysics
Branch:	High Energy Astrophysics
MSFC Colleague:	Charles A. Meegan
Date:	August 24, 1989
Contract No.:	The University of Alabama in Huntsville NGT-01-008-021

Abstract

MONTE CARLO MODELS AND ANALYSIS OF
GALACTIC DISK GAMMA-RAY BURST DISTRIBUTIONS

Jon Hakkila
Assistant Professor of Astronomy
Department of Mathematics, Astronomy, and Statistics
Mankato State University
Mankato, MN

Gamma-ray bursts are transient astronomical phenomena which have no quiescent counterparts in any region of the electromagnetic spectrum. Although temporal and spectral properties indicate that these events are likely energetic, their unknown spatial distribution complicates astrophysical interpretation.

Monte carlo samples of gamma-ray burst sources are created which belong to Galactic disk populations. Spatial analysis techniques are used to compare these samples to the observed distribution. From this, both quantitative and qualitative conclusions are drawn concerning allowed luminosity and spatial distributions of the actual sample.

Although the BATSE experiment on GRO will significantly improve knowledge of the gamma-ray burst source spatial characteristics within only a few months of launch, the analysis techniques described herein will not be superceded. Rather, they may be used with BATSE results to obtain detailed information about both the luminosity and spatial distributions of the sources.

Acknowledgements

I would particularly like to thank Charles Meegan for his guidance, assistance, and helpfulness on this enjoyable project, Jerry Fishman for inviting me here and for extending such warm hospitality, and Geoffrey Pendleton for introducing me to the wiles of monte carlo analysis. I would like to thank Gerald Karr, Frank Six, Billie Swinford, and the entire NASA/ASEE staff for coordinating such a fine and valuable program. I would also like to thank a few of the many people who made this summer more fun than a vacation could have been: Pat Lestrade, Tom Parnell, Ron Elsner, Bob Austin, Bob Wilson, Bill Pacesias, Scott Storey, Martin Brock, Charles Telesco, Roger Knacke, Stayce Harris, Philip Moore III, Jim Derrickson, John Watts, Ellen Roberts, Fred Berry Jr., and Peggy Champion. The FORTRAN function GAUSSD was written by Tom Jenkins of Case Western Reserve. Finally, I would like to thank my wife, Fahn, for sharing with me this wonderful summer in Huntsville.

Introduction

A. General Properties of Gamma-Ray Burst Sources

Since their discovery via examination of Vela satellite data records (Klebesadel, Strong, and Olson 1973), gamma-ray burst sources have remained one of the most enigmatic classes of objects in modern astronomy. The strong bursts of observed gamma-radiation that these objects emit have no quiescent counterparts at any other wavelength of the electromagnetic spectrum, and are at present of unknown origin. Multi-wavelength observations of the transient events are also unverified, although sporadic visible flashes have been reported (e.g. Schaefer 1981).

The burst durations range from $\tau < 0.1$ sec to $\tau > 100$ sec, although the majority apparently lie between 3 and 20 seconds (Hurley, unpublished). The events span a wide range of relative rise and decay times (Barat et al. 1984), although their general rapidity, as well as variations on timescales as short as milliseconds, suggest that at least some of the events must be associated with compact objects ($r < 10^3$ km). Since the events are time-integrated, the registered output is generally measured in fluence (erg cm^{-2}) instead of more conventional flux units (erg cm^{-2} sec^{-1}).

Although the peak burst power output lies between 150 and 500 keV for most bursts, the distribution (as observed from the KONUS catalogue) is sharply peaked around 200 keV (Higdon and Lingenfelter 1986). SMM observed hard high-energy tails, showing that burst power decreases at high energies (Nolan et al. 1984a). Burst power is also observed to turn over at low energies (e.g. Katoh et al. 1984). There are indications of cyclotron absorption features in the spectra from KONUS (Mazets et al. 1981), HEAO-A4 (Hueter et al. 1984), and GINGA (Murakami et al. 1988, Fenimore et al. 1989). Additionally, controversial observations of features thought to be positron-electron annihilation lines in emission have been made by KONUS (Mazets et al. 1981) and by SMM (Nolan et al 1984b).

B. Spatial Analyses of Burst Sources

The location of the burst sources in space is difficult to determine. Without prior knowledge of their luminosities, their observed fluxes cannot accurately be converted into spatial positions. Astrophysical models for the bursts must therefore remain vague until this controversy is resolved, as the burst sources might be local, disk-population Galactic, halo-population Galactic, or extragalactic in origin. There are two approaches by which this spatial distribution can be studied; (1) by examining the angular distribution of sources, (2) by examining the radial distribution of sources (such as is attempted using the log(N)-log(S) method or the V/V_{max} test).

1. The Angular Distribution of Sources

Angular spatial methods attempt to determine if the observed distribution prefers a position in space (such as the Galactic Center) or a symmetry plane (such as the ecliptic plane, the Galactic plane, or the plane containing the Local Supercluster of galaxies). Down to a minimum fluence of roughly 3×10^{-6} erg/cm^2, the spatial distribution of burst sources appears to be extremely isotropic (Mazets et al. 1981, Atteia et al. 1987). It also shows a negligible dipole moment, minimal quadrupole moments, and no propensity for clustering (Hartmann and Blumenthal 1988, Hartmann and Epstein 1989), in agreement with a random spatial distribution.

2. The Radial Distribution of Sources

a. Log(N)-Log(S) Curves

The number of sources N brighter than some fluence S provides one method by which the radial (distance) distribution of the sample can be measured. The luminosity distribution of a sample of sources with spatial density n in the luminosity interval (L,L+dL) is described by the luminosity function $\Phi(L)\ dL$. Functionally, $N(\geq S) = \int n\ V\ \Phi(L)\ dL$, and, since the fluence of a source decreases as r^2 (where r is the

distance to the source), $S = L/(4\pi r^2)$. For a uniform spatial distribution of sources (where the volume $V = [4\pi/3]\ r^3$), integration yields $N \propto S^{-3/2}$, or $\log(N) \propto -3/2\ \log(S)$. Similarly, a distance-limited sample will start off as $\log(N) \propto -3/2\ \log(S)$, but will turn over at faint fluence such that $\log(N) \propto 0$. A sample confined to the volume of a disk initially yields $\log(N) \propto -3/2\ \log(S)$; tilts over to become $\log(N) \propto -\log(S)$ at fainter fluence, and finally reaches $\log(N) \propto 0$ at faint fluence (when the disk has been completely sampled). A general description of log(N)-log(S) plots for disk models may be found in Fishman (1979).

Analysis of the log(N)-log(S) distribution of burst sources from early satellite catalogs (e.g. from KONUS, Mazets et al. 1981) indicates that the sample is in some way radially bounded, although this interpretation is quite controversial.

Higdon and Lingenfelter (1986) have noted that KONUS looks for bursts on low-energy (soft) channels, whereas some bursts apparently have stronger high-energy (hard) emissions. They suggest that the observed sample is biased to brighter (nearer) sources (as both hard and soft sources are detected at high fluence, whereas hard sources are more difficult for the equipment to trigger on if they are farther away), and argue that the corrected KONUS data is consistent with a log(N)-log(S) slope of -3/2. However, since the exact peak energy distribution (the relative number of soft to hard sources) is unknown, the amount of correction applied to obtain these results is quite model-dependent.

Since the detectors used trigger on minimum flux rather than on minimum fluence, they are more likely to sense short bursts than long ones. Although many observers suggest that the raw peak photon rate C should be used instead of fluence to bypass detector response, the overall problem of interpretation still remains unresolved. Paczynskii and Long (1986) infer that the faint-end log(N)-log(C) slope is -1.07 (indicating a radial limit in agreement with a Galactic disk model), while Jennings (1982,1984) corrects the data to a slope of -3/2.

Meegan et al. (1985) have placed an upper limit on the log(N)-log(S) curve from balloon data. Their analysis incorporates (1) calculation of a detector count-rate triggering threshold, (2) conversion of this rate threshold to a fluence threshold, (3) simulations of the fraction of incident photons that will trigger each detector, (4) corrections for temporal triggering effects, and (5) analysis of the distribution based upon assumed spectral shapes of bursts. Their results indicate an upper limit of 2300 bursts/year at a fluence of 6×10^{-7} erg cm^{-2}. In order to fall below this limit, the log(N)-log(S) curve must turn over below 10^{-4} erg cm^{-2}.

b. The Radial/Angular Distribution of Sources

Schmidt (1968) developed another statistical test which analyzes the radial distributions of an astronomical sample, known as the V/V_{max} test. This test is based upon the instrumental parameters C_{Lim} (the limiting count rate for a detector) and C_S (the source's observed count rate). For a uniformly-distributed sample, the count rate of a source depends upon its distance R_S. Since the limiting count rate corresponds the the distance Rmax that the source would have with count rate C_{Lim}, $R_{max} = R\ (C_S/C_{Lim})^{1/2}$, and $V/V_{max} = (C_S/C_{Lim})^{-3/2}$. For a sample of sources, the average value $\langle V/V_{max} \rangle = \int_1^\infty (C_S/C_{Lim})^{-3/2}$ $d(C_S/C_{Lim}) = 1/2$. Thus, a sample with $\langle V/V_{max} \rangle < 1/2$ is distributed preferentially nearby, whereas one with $\langle V/V_{max} \rangle > 1/2$ is located preferentially far away. Schmidt, Higdon, and Hueter (1988) have used the V/V_{max} test on 13 HEAO-A4 gamma-ray bursts (with varying values of C_{Lim}) to indicate that $\langle V/V_{max} \rangle = 0.40 \pm 0.08$, which they point out is consistent with uniformity. However, this value is also consistent with the beginnings of a log(N)-log(C) turnover.

C. Astrophysical Models of Burst Sources

Many astrophysical models exist for gamma-ray burst production, and are summarized in reviews by Liang (1989) and Hurley (1989). Possible models include compact sources in the cores of active galactic nuclei, massive galaxies, and globular clusters. However, the short timescale variability, cyclotron absorption features, and possible redshifted positron-electron annihilation lines in burst spectra lead to a favored model; that of a neutron star emitting by (1) accreting material and flashing, (2) vibration, (3) undergoing a crustquake, (4) being resurrected as a pulsar, or (5) via a magnetic flare. The limited power outputs of neutron star models suggest that a turnover in the log(N)-log(S) curve should be visible at some point.

Objectives

Accurate models of the gamma-ray burst distribution are not obtained simply. Direct integrations of log(N)-log(S) and angular functions describing the distribution are generally quite difficult to perform. Also, the functional forms of these distributions are quite model-dependent, so direct integration of a great number of possible distributions is needed. This makes the problem even more unwieldy.

Monte carlo techniques eliminate the difficulties of direct integration while simultaneously allowing great freedom in examining model parameters. By creating a variety of discrete sources randomly, radial and angular distributions may be examined and compared to those of the actual data set. New models are easily created by merely adjusting model parameters. Models which are obviously incompatible with the observed data can be eliminated, while statistical tests performed on compatible models place restrictions on allowed parameter values.

For this project, a Galactic disk spatial distribution is chosen for the sources (halo models can be easily incorporated in the future, although the log(N)-log(S) distributions of these models do not apparently turn over fast enough at low fluence). A variety of source luminosity functions are tested within this framework, so that models with unreasonable luminosity functions might be eliminated.

A Monte Carlo Model of Galactic Disk Sources

The procedure used to test the validity of a model is to (1) choose model parameters from which a monte carlo data set is generated, (2) select only those generated sources which have fluences bright enough to be measured, and (3) statistically compare the radial and angular properties of the artificial data set with the real one. A number of these models can be eliminated from consideration. Finally, general luminosity and spatial properties of the real data may be inferred from the monte carlo models. Creation of the monte carlo data set is carried out via program GAMMA.FOR (figure 1), and the data analysis is performed by program GAMMA.PRO.

A. General Model Parameters

The general model parameters are allowed to be changed within the program, and it is in fact not difficult to change the functional forms of any parameters. The gamma ray bursts are assumed to originate on Galactic neutron stars, so the spatial distribution is that of the Galactic disk. Model parameters describing the Galactic disk are taken from the book *Galactic Astronomy*, by Mihalas and Binney (1981), and are meant to mimic general properties of the Milky Way (as presently understood). These values may, however, be varied easily within the program. A variety of luminosity functions are also allowed in the model, and parameters describing these functions may be easily changed.

1. The Three-Dimensional Galactic Disk

This disk model is intended to represent a variety of stellar ages and populations, but the youngest disk (spiral arm) population has been purposefully overlooked because the spatial distribution of bursts is apparently too isotropic to be associated with (1) spiral arms, and (2) a tendency to cluster as is observed for the youngest objects.

The Galactic disk is therefore characterized
(1) in the Θ-direction by an isotropic distribution (i.e. there are

no angular structures such as spiral arms).

(2) in the z-direction (perpendicular to the Galactic plane) by a Gaussian distribution. There are physical reasons for choosing this model over either a linearly- or an exponentially-decreasing one (although both of these are often used in Galactic astronomy): Primarily, these models exhibit discontinuities at z = 0, whereas a Gaussian model does not. Furthermore, these models are not as easy to explain in terms of maintenance via a Galactic gravitational potential. The width of the Gaussian distribution is represented by the variance σ_z^2, where σ_z differs from the exponential scale height by $\sqrt{2}$. Choosing a value for σ_z is difficult. Scale heights of stellar populations are estimated from Mihalas and Binney (1981) p. 278, to be as follows: Spiral Arm population (age $\leq 10^8$ years) = 120 parsecs, Young disk population (age $\approx 10^9$ years) = 200 parsecs, Intermediate disk population (age $\approx 5 \times 10^9$ years) = 400 parsecs, and Old Disk population (age $\leq 10^{10}$ years) = 700 parsecs. A disk sample with a constant birthrate function would have an average age of around 5×10^9 years (if the disk is 10^{10} years old), and a scale height of roughly 400 parsecs. This might be an underestimate, as the suspected scale height of white dwarf stars is 500 parsecs. A best guess value for σ_z is therefore 350 parsecs, corresponding to a scale height of 500 parsecs.

(3) in the r-direction (radially outward from the Galactic center) by an exponentially-decreasing density function. This is both observed locally and from brightness distributions of other spiral galaxies of similar Hubble types. This exponential decrease is convolved with the infinitesimal radial increase ($r \times dr$) needed to keep a constant disk density for cylindrical geometry. The exponential scaling factor R_S of the distribution $\exp(-r/R_S)$ is obtained from scaling the size of the Milky Way Galaxy to that of the Andromeda Galaxy (M31), and is therefore $R_S = 3.9$ kpc.

The sun is assumed to lie at a distance of 8.5 kpc from the Galactic center, in the Galactic plane.

2. The Luminosity Function of Burst Sources

Several "standard" luminosity functions of burst sources are allowed:

(1) All sources have the same luminosity, <L>.

(2) The sources are chosen from a Gaussian luminosity function characterized by <L> and σ_L.

(3) The sources are chosen from a topheavy luminosity function linearly increasing in number between L_{min} and L_{max}.

(4) The sources are chosen from a bottomheavy luminosity function linearly decreasing in number between L_{min} and L_{max}.

(5) The sources are selected from a bottomheavy power law luminosity function where $N(L) \propto (L/L_{min})^{-\alpha}$.

A sample of the modeled disk distribution (for sources of a single luminosity <L>) is shown in figure 3.

B. Selection of Data for Analysis

Once each "burst" has been given a Galactic position and a luminosity, fluences and observed positions for it (in Galactic coordinates *l* and *b*) are calculated. Only those sources with fluences greater than S_{min} are selected (S_{min} is chosen to be 2×10^{-7} erg cm^{-2}, as this represents a minimum value of log(S) for which reliable log(N) data exists). From these data, a log(N)-log(S) array is built and angular characteristics are examined. An estimate must be made of the total number of sources, since this in part determines the "goodness of fit" of the log(N)-log(S) plot. At present this fit is estimated by inspection; future work may introduce a subroutine which optimizes the number of sources used.

It should be noted that Galactic disk samples of low-luminosity sources take much more CPU time to create than those of high-luminosity sources. This is due to the sample's (disk height/limiting distance) ratio, which is larger for low-luminosity sources than it is for high-luminosity ones. In other words, the luminous sources are confined to an almost two-dimensional flat disk (which the computer rapidly fills), whereas the low-luminosity ones are confined within a three-dimensional sphere (which fills in more CPU time).

Samples with a range of luminosities (such as the power law luminosity distribution described above) also use larger amounts of CPU time, which sometimes can be prohibitively large on a small computer such as a VAX.

C. Method of Data Analysis

The log(N)-log(S) curve is produced from the data, and is chosen to (1) match the log(N)-log(S) plot observed from satellite data at high fluence, and (2) stay below the balloon limit (Meegan et al. 1985) of 2300 bursts/year at a fluence of 6×10^{-7} erg cm^{-2}. The slope d[log(N)/log(S)]/d[log(S)] is also compared to that of the actual data set.

The spatial distribution can be plotted for any minimum fluence in Galactic coordinates *l* and *b*. A quick-and-dirty analysis checks the distribution of events brighter than this minimum fluence as a function of Galactic latitude region by considering three latitude regions of equal area. The Galactic latitude regions $0° \leq |b| \leq 19.5°$ (low-latitude), $19.5° < |b| \leq 41.8°$ (mid-latitude), and $41.8° < |b| \leq 90°$ (high-latitude), should contain equal numbers of stars n, with errors $n/\sqrt{(n-1)}$. A more accurate method of analysis is also presented, as the system's dipole and quadrupole moments are calculated. A large dipole moment indicates that the distribution is biased towards one direction. The quadrupole moments yield two useful parameters: η (the difference between the two closest eigenvalues of the quadrupole tensor) and ζ (the most different eigenvalue). When $\eta = \zeta = 0$, the distribution is isotropic. An oblate (disk) distribution is indicated by $\zeta \geq 0$, whereas a prolate distribution (one which is strongly bipolar) is indicated by $\zeta \leq 0$.

D. Results of Preliminary Data Analysis

Samples of program output and data analysis are shown in figures 4, 5, and 6. Once a number of models have been run, a comparison can be made between them and the actual data.

The constraints imposed by both an isotropic angular distribution for high minimum fluence ($S_{min} \geq 3 \times 10^{-6}$ erg cm^{-2}) and an apparent turnover in the log(N)-log(S) curve turn out to be quite strict. For $\sigma_z = 400$ parsecs and a single luminosity function L = <L>, a lower luminosity limit of $<L> \approx 4 \times 10^5$ solar luminosities or 1.5×10^{39} erg is necessary to turn the log(N)-log(S) curve over by $S = 2 \times 10^{-5}$ erg cm^{-2} (the "elbow", or the lowest fluence where the log(N)-log(S) curve can turn over in order to stay below the balloon data limit with a physically meaningful slope). Models with lower average luminosities do not stay below the balloon data log(N) upper limit. Those with

higher average luminosities effectively stay below the balloon limit, but do not match the log(N)-log(S) curve at high fluence, do not show spatial isotropy for minimum fluences below that of the "elbow", and predict a Galactic radius exceeding 15 kpc (compared to the apparent radius of 13.5 kpc). Thus only a small range of average luminosities between these extremes satisfies the observations, and the model is strongly constrained.

Many implications arise from these limits:

(1) The spatial density of sources is somewhere around 3×10^{-8} pc^{-3} yr^{-1}. If there are roughly 3×10^{7} neutron stars in the Galaxy (Hartmann, Epstein, and Woosley 1989), then the bursts sources must repeat on an average of around 10^{5} years to explain the burst rate.

(2) The range of acceptable luminosities is too high for existing astrophysical models of neutron star crustquakes or resurrected pulsars (see Liang 1989), suggesting that these models are unlikely.

(3) The effects of other luminosity functions on the results are not very pronounced. A Gaussian function broadens the "elbow" from a well-defined point to a curve and strengthens any spatial anisotropies that are present, due to an oversampling of the luminous sources (see also Hakkila 1989). The topheavy and bottomheavy functions, being linear, exhibit slight effects that are very similar to the Gaussian distribution, although the bottomheavy function tends to show more spatial isotropy at high fluence. The power law function is the most promising luminosity function, but at present consumes an inordinate amount of CPU time.

Conclusions and Recommendations

A. Conclusions

This approach appears to provide a useful method for analyzing the properties of gamma-ray burst sources, as well as for analyzing properties of other astronomical objects. Detailed analysis which include interstellar absorption could lead to a better understanding of Galactic structure, stellar populations, and stellar evolution.

Observations of gamma-ray bursts (angular isotropy at high fluence coupled with a log(N)-log(S) turnover) strongly constrain the number and types of allowed monte carlo simulations. The allowed models suggest that, for a distribution characterized by a single source luminosity <L>, only a small range of luminosities (10^{39} erg $\leq$ <L> $\leq$ 6×10^{39} erg) result in acceptable fits to the actual data. Other luminosity functions do not significantly alter these general conclusions, although the effects of bottomheavy power law functions are still unknown (due to prohibitive use of CPU time).

The implications of these results are worrisome, as they indicate that (1) some of the observational data is in error, (2) selection effects are still present in the existing data, (3) the Galactic disk model used in this monte carlo analysis is significantly in error, (4) a Galactic disk model is not the proper representation for the distribution of gamma-ray burst sources, or (5) the bursts really all have only a small luminosity range.

B. Recommendations

This approach is still only in the preliminary stages. More work still needs to be done in order to

(1) quantify the comparison between models and observations,
(2) vary disk parameters in order to see what effects different stellar populations have upon the resultant distributions,
(3) examine the effects of a Galactic halo component,
(4) integrate models over larger data samples to get better statistics,
(5) include a method for optimizing the number of generated

sources,

(6) study the effects of a bottomheavy power-law luminosity function,

(7) refine the Galactic model to incorporate new understanding about Galactic structure,

(8) prepare for the possibility the BATSE will identify burst subpopulations, as these will then have to be examined separately,

(9) etc.

Of course, the new data obtained from the BATSE experiment on GRO should resolve the bulk of the burst distribution problem within only a few months of launch, and the data set that it generates can help isolate the locations of and mechanisms responsible for the gamma-ray burst sources. With the BATSE data, methods such as this will prove useful in isolating (1) the luminosity function of the burst sources, and (2) the stellar population of the burst sources (should they prove to have Galactic origins).

References

Atteia, J.-L. et al. 1987, *Ap. J. Supp. Ser.* **64**, 305.
Barat, C. et al. 1984, *Ap. J.* **285**, 791.
Fenimore, E. et al. 1989, *Ap. J.* submitted.
Fishman, G. J. 1979, *Ap. J.* **233**, 851.
Hakkila, J. 1989, *Ap. J.* in press.
Hartmann, D., and Epstein, R. I. 1988, *Ap. J.* in press.
Hartmann, D., Epstein, R. I., and Woosley, S.E. 1989, *Nucl. Phys. B.* in press.
Hartmann, D., and Blumenthal, G. 1989, *Ap. J.* submitted.
Higdon, J., and Lingenfelter, R. 1986, *Ap. J.* **307**, 197.
Hueter, J. 1987, Ph. D. Dissertation, U. C. San Diego.
Hurley, K. 1989, *Proc. NATO ASI Erice School on Cosmic Rays*, ed. Shapiro, M. M. (Dordrecht: Reidel).
Jennings, M. C. 1982, *Ap. J.* **258**, 110.
Jennings, M. C. 1984, AIP Conf. Proc. No. 115, ed. Woosley, S. E. (New York: AIP Press), p. 412.
Katoh et al. 1984, AIP Conf. Proc. No. 115, ed. Woosley, S. E. (New York: AIP Press), p. 390.
Klebesadel, R. W., Strong, I., and Olson, R. 1973, *Ap. J. (Letters)* **182**, L85.
Liang, E. P. 1989, preprint.
Mazets, E. P., et al. 1981, *Ap. Sp. Sci.* **80**, 3.
Meegan, C. A., Fishman, G. J., and Wilson, R. B. 1985, *Ap. J.* **291**, 479.
Mihalas, D., and Binney, J. 1981, *Galactic Astronomy: Stucture and Kinematics* (San Francisco: W. H. Freeman).
Murakami, T. et al. 1988. *Nature* **335**, 234.
Nolan, P. L. et al. 1984a, AIP Conf. Proc. No. 115, ed. Woosley, S. E. (New York: AIP Press), p. 399.
Nolan, P. L. et al. 1984b, *Nature* **311**, 360.
Paczynskii, B., and Long, K. 1988, *Ap. J.* **301**, 213.
Schaefer, B. 1981, *Nature* **294**, 722.
Schmidt, M. 1968, *Ap. J.* **151**, 393.
Schmidt, M., Higdon, J. C., and Hueter, G. 1988, *Ap. J. (Letters)* **329**, L85.

ORIGINAL PAGE IS
OF POOR QUALITY

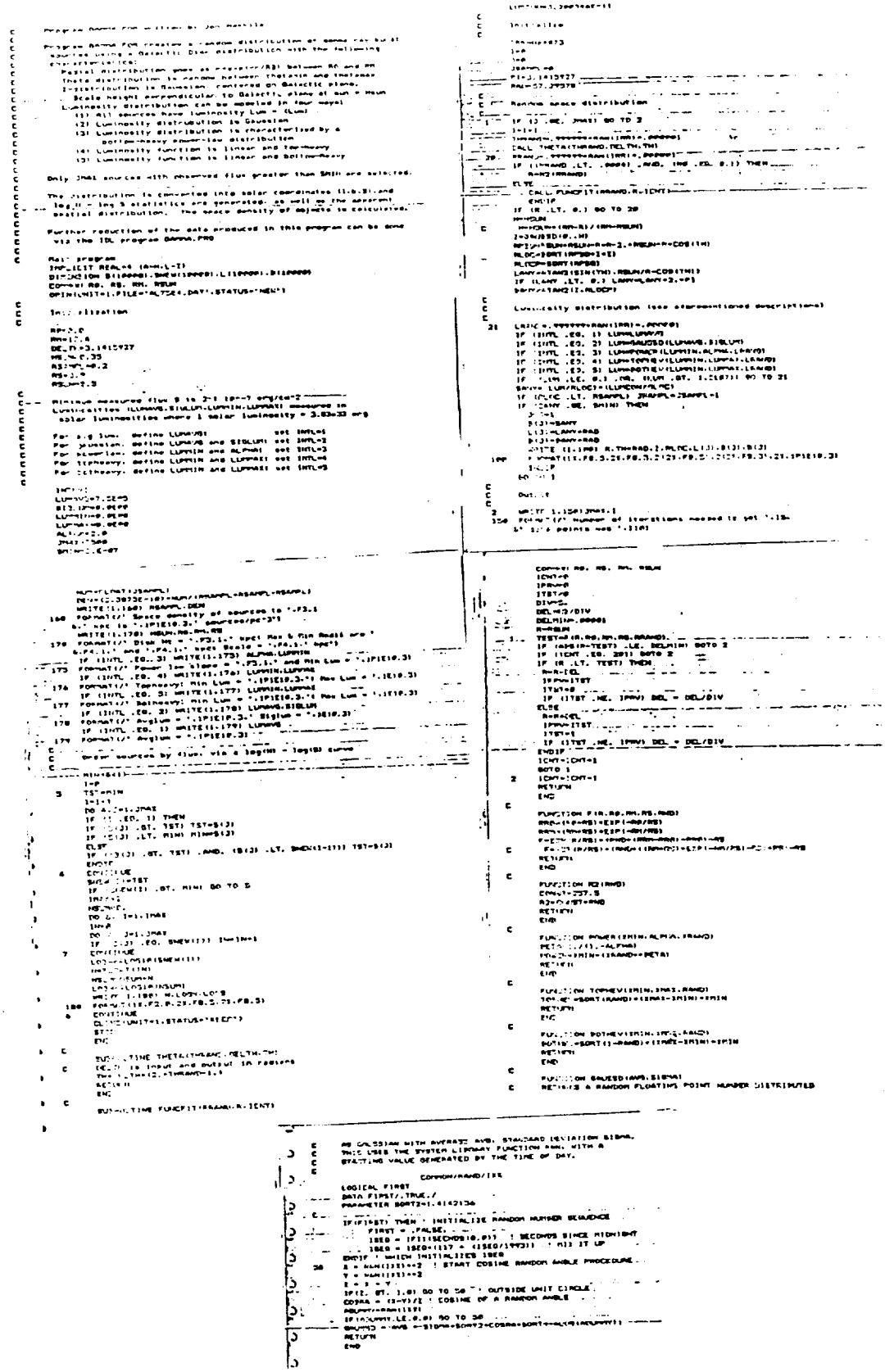

Figure 1. The computer program GAMMA.FOR used to generate the monte carlo data sets.

ORIGINAL PAGE IS
OF POOR QUALITY

```
;       IDL program GAMMA.PRO written by Jon Hakkila
;
;       Program GAMMA.PRO analyses output from GAMMA.FOR, producing
;        four (4) plots and one (1) output file (GAMMA.OUT).
;       Parameters which need to be set in this program are the input
;        file's name, the total number of sources created (JTOT) (identical
;        to JMAX in GAMMA.FOR), JM (the number of logN entries, which can
;        be obtained from the input file's total number of lines NUM as
;        JM=NUM-JMAX-8), STST (a minimum flux), and !MTITLE (the desired
;        main title for the plots).
;       The program plots a logN-logS curve for the monte Carlo data and
;        compares it to observations. It also plots the slope of this line
;        d logN/d logS as a function of logS. The total distribution is then
;        spatially sampled for four minimum fluences: 10^-6, 10^-5, 10^-4,
;        and STST.  For each of these a latitude distribution of the data
;        (divided into three equal area on the sky in Galactic coordinates
;        l and b) is obtained, and is compared to that of a random distribution.
;        Also calculated are the dipole and quadrupole moments of the
;        distributions, which should be zero for a randomly distributed
;        sample.
;       Additional variables which can be easily set in this program are JMIN
;        (the smallest value of N to be used in calculating d logN/d logS)
;        and NPTS (the number of equal-sized logS divisions that will be used
;        in this calculation. A "divide-by-zero" error is generally corrected
;        either by slightly raising JMIN or lowering NPTS.
;
OPENR,1,'AL7SE4.DAT'
OPENW,2,'GAMMA.OUT'
!MTITLE='Avg Lum Dist: Lavg=7.5E5 Lsun'
JM=7497
STST=2.0E-05
JTOT=7500
JMIN=5
NPTS=22
STN=STRAT(0,10,0)
SMIN=FLTARR(4) & SMIN([0,1,2,3])=[1.0E-06,1.0E-05,1.0E-04,STST]
PCT=FLTARR(3)  & A=FLTARR(7,JTOT) & C=FLTARR(3,JM)
LSDAT =FLTARR(3) & LSDAT([0,1,2])    =[-6.222,-4.70,-3.42]
LNDAT =FLTARR(3) & LNDAT([0,1,2])    =[3.362,1.58,0.00]
NEWSDT=FLTARR(4) & NEWSDT([0,1,2,3])=[-6.22,-5.22,-4.70,-3.70]
SLPDT =FLTARR(4) & SLPDT([0,1,2,3]) =[-1.,-1.,-1.5,-1.5]
CNTA  =FLTARR(3) & CNTA([0,1,2])     =[0.0,2.0,4.0]
AVG   =FLTARR(3) & AVG(*)            =0.333333
CNT   =FLTARR(3) & CNT([0,1,2])      =[1.,2.,3.]
PE1 =FLTARR(2) & PE2 =FLTARR(2) & PE3 =FLTARR(2)
CNT1=FLTARR(2) & CNT1([0,1])=[0.999999,1.00000]
CNT2=FLTARR(2) & CNT2([0,1])=[1.999999,2.00000]
CNT3=FLTARR(2) & CNT3([0,1])=[2.999999,3.00000]
IND=INTARR(NPTS) & SLOPE=FLTARR(NPTS)   & NEWS=FLTARR(NPTS)
DTHE  =FLTARR(JTOT) & DPHI=FLTARR(JTOT)
DX    =FLTARR(JTOT) & DY  =FLTARR(JTOT) & DZ=FLTARR(JTOT)
DIFCOM=FLTARR(3)     & DIFF=FLTARR(3)     & ZETA=FLTARR(3)
READF,1,?
READF,1,STN
READF,1,C
CLOSE,1
X=A(0,*)*SIN(A(1,*)/57.29578) & Y=A(0,*)*COS(A(1,*)/57.29578)
Z=A(2,*) & T=A(3,*) & L=A(4,*) & B=A(5,*) & S=A(6,*)
L(WHERE(L GT 180.)) = L(WHERE(L GT 180.))-360.
LOGN=C(1,*)
LOGS=C(2,*)
DLS=(LOGS(JM-1)-LOGS(JMIN))/NPTS
PRINTF,2,'(A)','        MONTE CARLO DISTRIBUTION OF GAMMA-RAY BURST SOURCES'//)'
PRINTF,2,'(A)','MODEL PARAMETERS')'
PRINTF,2,'(A80)',STN
PRINTF,2,'(///'LOGN-LOGS SUMMARY'//'Index   # Pts     LogN      LogS'/)'
FOR J=0,NPTS-1 DO BEGIN
  T=LOGS(JMIN)+J*DLS
  I=0
  REPEAT I=I+1 UNTIL (((LOGS(I) GT T) AND (LOGS(I+1) LE T)) OR (I GE (JM-1)))
  IND(J)=I
  PRINTF,2,'(2(I5,2X),2(F7.3,2X))',J,IND(J)+1,LOGN(IND(J)),LOGS(IND(J))
  IF (J GT 0) THEN BEGIN
    DLOGN=LOGN(IND(J))-LOGN(IND(J-1))
    DLOGS=LOGS(IND(J))-LOGS(IND(J-1))
    SLOPE(J-1)=DLOGN/DLOGS
    NEWS(J-1) =LOGS(IND(J-1))+DLOGS/2.
  ENDIF
ENDFOR
DLOGN=LOGN(JM-1)-LOGN(IND(NPTS-1))
DLOGS=LOGS(JM-1)-LOGS(IND(NPTS-1))
SLOPE(NPTS-1)=DLOGN/DLOGS
NEWS(NPTS-1) =LOGS(IND(NPTS-1))+DLOGS/2.
PRINTF,2,'(2(I5,2X),2(F7.3,2X))',NPTS,JM,LOGN(JM-1),LOGS(JM-1)
PRINTF,2,'(///'SPACE DISTRIBUTION PROPERTIES'/)'
FOR II=0,3 DO BEGIN
 HLAT=N_ELEMENTS(WHERE((ABS(B) GT 41.81) AND (S GE SMIN(II))))
 IF (!ERR EQ 0) THEN HLAT=0
 TOTA=N_ELEMENTS(WHERE(S GE SMIN(II)))
 IF (!ERR EQ 0) THEN TOTA=0
 LLAT=N_ELEMENTS(WHERE((ABS(B) LE 19.47) AND (S GE SMIN(II))))
 IF (!ERR EQ 0) THEN LLAT=0
 MLAT=TOTA-HLAT-LLAT
 PTS=HLAT+MLAT+LLAT
 ELAT=(PTS/3.)/SQRT(PTS/3.-0.33333)
 PCT(0)=LLAT*1./PTS & PCT(1)=MLAT*1./PTS & PCT(2)=HLAT*1./PTS
 PRINTF,2,'(A10,1PE9.2,A10,I5,A8,F8.1,A5,F5.1)','Min. Flux: ',SMIN(II), $
  '  Total = ',PTS,'  Avg = ',PTS/3.,' +/- ',ELAT
 PRINTF,2,'(7X,3(2X,I5,A2,F6.2,A2))',LLAT,' (',100.*PCT(0),')',MLAT, $
  ' (',100.*PCT(1),')',HLAT,' (',100.*PCT(2),')'
 PE1([0,1])=[(LLAT+ELAT)/PTS,(LLAT-ELAT)/PTS]
 PE2([0,1])=[(MLAT+ELAT)/PTS,(MLAT-ELAT)/PTS]
 PE3([0,1])=[(HLAT+ELAT)/PTS,(HLAT-ELAT)/PTS]
 DTHE=(90.-B(WHERE(S GE SMIN(II))))/57.2958
 DPHI=L(WHERE(S GE SMIN(II)))/57.2958
 DX=SIN(DTHE)*SIN(DPHI) & DY=SIN(DTHE)*COS(DPHI) & DZ=COS(DTHE)
 DX(WHERE(ABS(DX) LT 1.E-05))=0. & DY(WHERE(ABS(DY) LT 1.E-05))=0.
 DZ(WHERE(ABS(DZ) LT 1.E-05))=0.
 DAVGX=TOTAL(DX)/JTOT    & DAVGY=TOTAL(DY)/JTOT    & DAVGZ=TOTAL(DZ)/JTOT
; PRINTF,2,'(3(2X,F8.5))',DX,DY,DZ
; PRINTF,2,'(3(3X,F8.5))',DAVGX,DAVGY,DAVGZ
 DR=SQRT(DAVGX*DAVGX+DAVGY*DAVGY+DAVGZ*DAVGZ)
 SIGDIP=1./SQRT(3.*PTS-1.)
 DL=ATAN(DAVGX,DAVGY)*57.2958
 DB=57.2958*ATAN(DAVGZ,SQRT(DAVGX*DAVGX+DAVGY*DAVGY))
 PRINTF,2,'(/2X,A8,F5.3,A8,F7.2,A5,F6.2)','DIPOLE: ',DR, $
  ' at l= ',DL,' and b = ',DB
; PRINTF,2,'(/2X,A8,F5.3,A5,F5.3,A8,F7.2,A9,F6.2)','DIPOLE: ',DR, $
;  ' +/- ',SIGDIP,' at  l= ',DL,' and  b= ',DB
 QXX=TOTAL(3.*DX*DX-1.)/JTOT & QXY=TOTAL(3.*DX*DY)/JTOT
 QYY=TOTAL(3.*DY*DY-1.)/JTOT & QXZ=TOTAL(3.*DX*DZ)/JTOT
 QZZ=TOTAL(3.*DZ*DZ-1.)/JTOT & QYZ=TOTAL(3.*DY*DZ)/JTOT
; PRINTF,2,'(3(2X,F5.2))',QXX,QXY,QXZ
; PRINTF,2,'(3(2X,F5.2))',QXY,QYY,QYZ
; PRINTF,2,'(3(2X,F5.2))',QXZ,QYZ,QZZ
 P=QXX*QYY+QZZ*QXX+QYY*QZZ-QXY*QXY-QYZ*QYZ-QXZ*QXZ
 Q=QXX*QYZ*QYZ+QYY*QXZ*QXZ+QZZ*QXY*QXY-QXX*QYY*QZZ-2.*QXY*QXZ*QYZ
 DISC=P*P*P/27.+Q*Q/4.
 IF DISC GT 0. THEN BEGIN & ETA=0. & ZETA=0. & GOTO,JUMP & ENDIF
 PSI =ACOS((-Q/2.)*((ABS(P)/3.)^(-1.5)))
 EIG1=-2.*SQRT(ABS(P)/3.)*COS(PSI/3.)
 EIG2= 2.*SQRT(ABS(P)/3.)*COS(PSI/3.-1.0471976)
 EIG3= 2.*SQRT(ABS(P)/3.)*COS(PSI/3.+1.0471976)
 DIFCOM([0,1,2])=[EIG3,EIG2,EIG1]
 DIFF([0,1,2])  =[ABS(EIG1-EIG2),ABS(EIG1-EIG3),ABS(EIG2-EIG3)]
 ETA =MIN(DIFF) & !C=0 & ZETA=DIFCOM(ETA EQ MIN(DIFF)) & !C=0
 SIGETA=SQRT(2.)*SIGDIP & SIGZET=SIGDIP
 JUMP: PRINTF,2,'(2X,A10,F5.3,A9,F5.3/)','QUADRUPOLE:  eta= ',$
 ETA,'  zeta= ',ZETA
; JUMP: PRINTF,2,'(2X,A10,F5.3,A5,F5.3,A9,F5.3,A5,F5.3/)', $
; 'QUADRUPOLE:  eta= ',ETA,' +/- ',SIGETA,'  zeta= ',ZETA,' +/- ',SIGZET
 ENDFOR
CLOSE,2
SET_PLOT,2
!PSYM=10
!TYPE=16
!FANCY=2
!XTITLE='log(S)'
!YTITLE='log(N)'
PLOT,LOGS,LOGN
!PSYM=0
!LINETYPE=2
OPLOT,LSDAT,LNDAT
!LINETYPE=0
!PSYM=1
!YTITLE='d log(N)/d log(S)'
PLOT,NEWS,SLOPE
!IGNORE=1
!PSYM=5
OPLOT,NEWSDT,SLPDT
!PSYM=0
!XTITLE='Galactic Latitude Region'
!YTITLE='Percentage of Objects'
!YMIN=0.
!YMAX=1.
PLOT,CNTA,AVG
!PSYM=2
OPLOT,CNT,PCT
!PSYM=0
!IGNORE=0
OPLOT,CNT1,PE1
OPLOT,CNT2,PE2
OPLOT,CNT3,PE3
!PSYM=3
!YMIN=-90
!YMAX=90
!XTITLE='Galactic Longitude'
!YTITLE='Galactic Latitude'
PLOT,L(WHERE(S GE STST)),B(WHERE(S GE STST))
END
```

Figure 2. The computer program GAMMA.PRO used to analyze the monte carlo data sets.

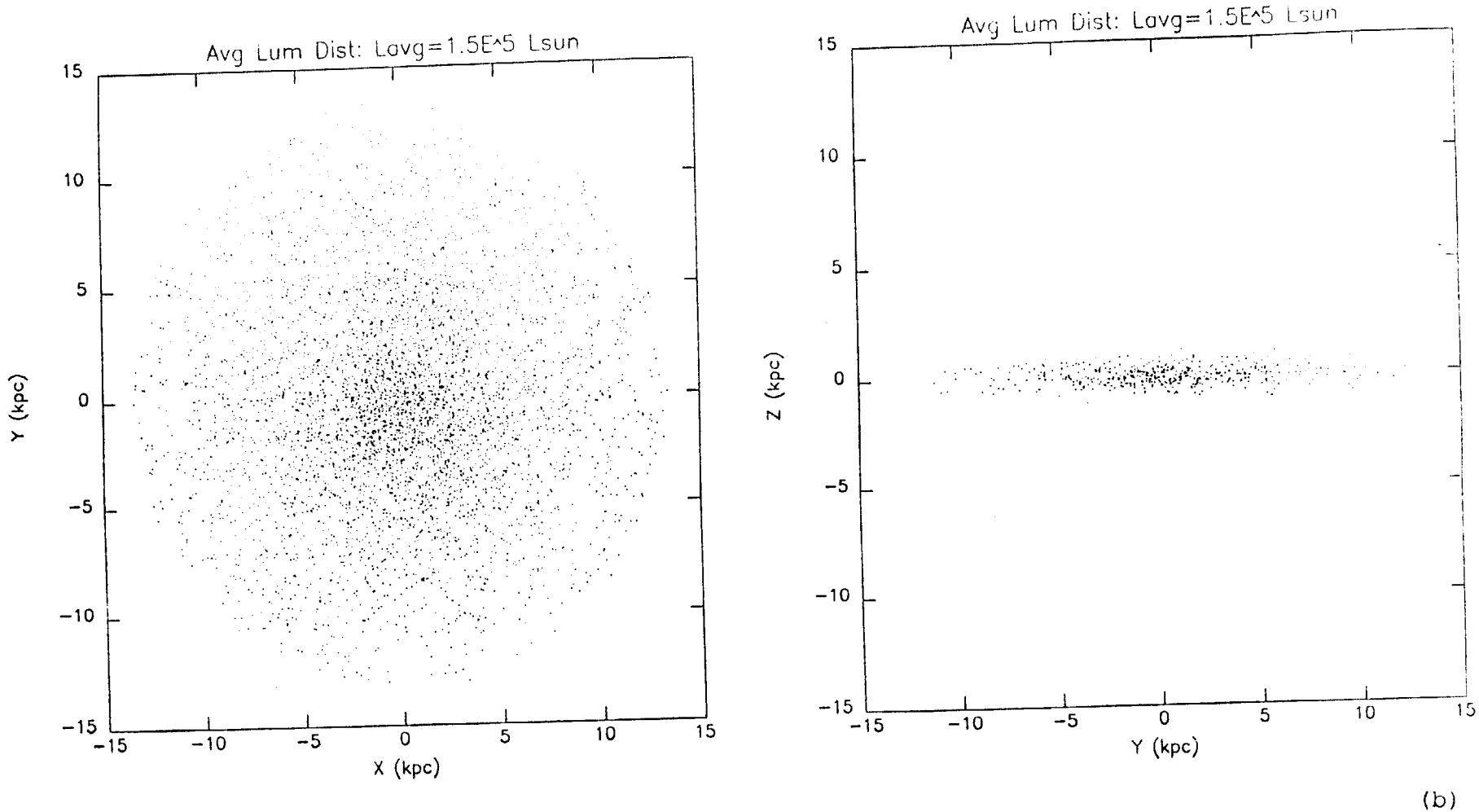

Figure 3. An example of the disk distribution produced by monte carlo analysis. This disk, with a radius of 13.5 kpc and a width of 400 pc, is shown (a) from above, and (b) looking at a band 1 kpc wide running across its diameter.

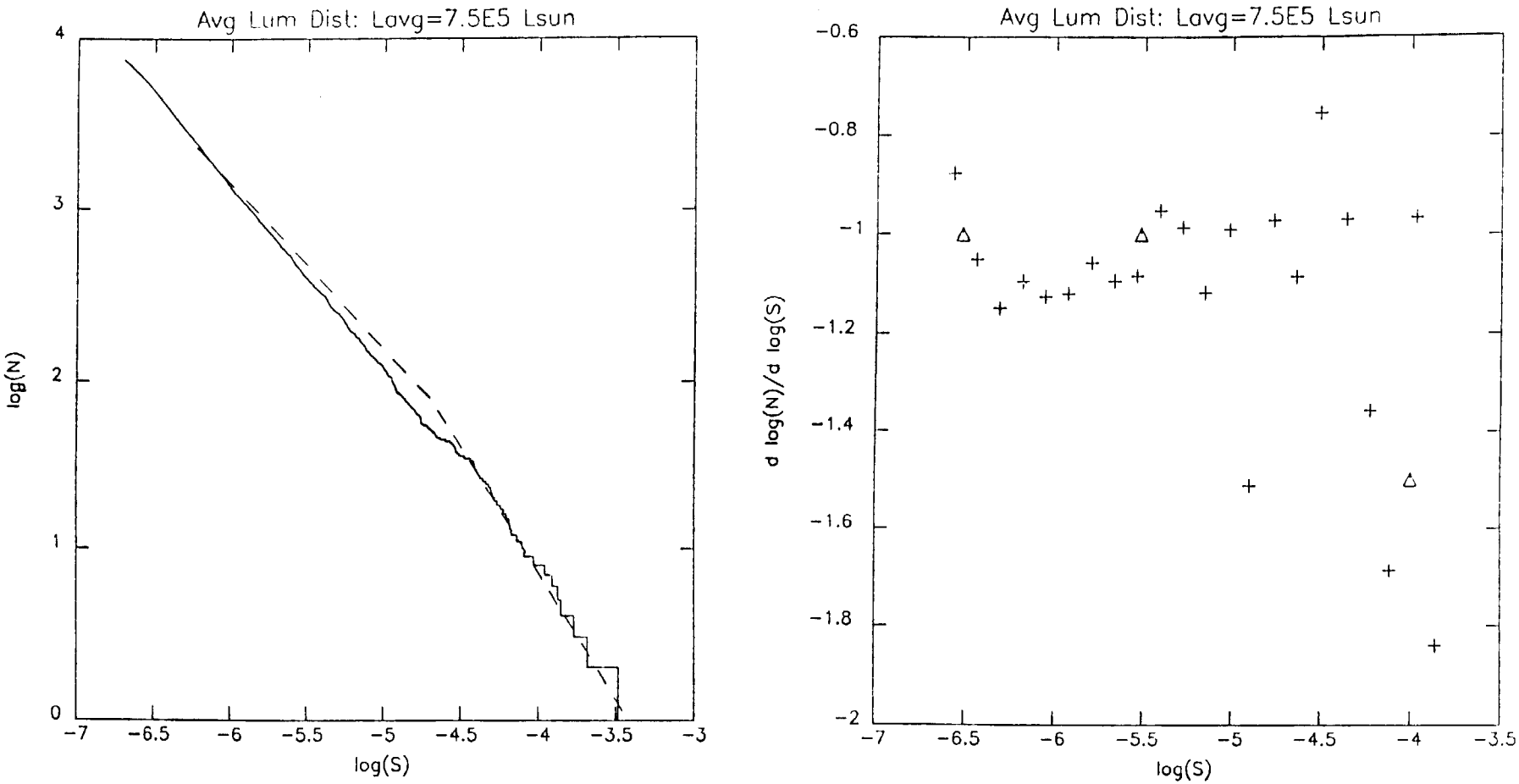

Figure 4. Log(N)-log(S) results for a sample of 7500 observed sources with luminosity <L> = 7.5×10^5 Lsun = 3×10^{39} erg cm^{-2}. The log(N)-log(S) plot (which fits the observed data) is shown in (a). The high-fluence end of the dotted line depicts satellite data, while the low-fluence end is an upper limit based upon the balloon observations of Meegan et al. (1985). Log(N)-log(S) slopes from balloon and satellite data (triangles), are compared to those of the monte carlo analysis (crosses) in (b).

```
                    MONTE CARLO DISTRIBUTION OF GAMMA-RAY BURST SOURCES

MODEL PARAMETERS

 Number of iterations needed to get  7500 data points was        13340

 Space density of sources to 0.2 kpc is  2.230E-04 sources/pc^3

 Disk ht  0.4 kpc; max & min radii are  0.0  and 20.1 kpc; scale =  3.9 kpc

 Avglum =  5.500E+05 siglum =  0.000E+00


LOGN-LOGS SUMMARY

Index   # of s      LogN      LogS

    0       7      0.699    -3.862
    1       8      0.903    -3.972
    2      11      1.041    -4.116
    3      17      1.230    -4.228
    4      26      1.415    -4.361
    5      36      1.556    -4.509
    6      45      1.653    -4.638
    7      62      1.792    -4.764
    8      83      1.919    -4.896
    9     127      2.104    -5.010
   10     174      2.241    -5.156
   11     239      2.384    -5.281
   12     324      2.511    -5.413
   13     429      2.633    -5.542
   14     572      2.772    -5.670
   15     784      2.914    -5.798
   16    1082      3.050    -5.920
   17    1482      3.194    -6.056
   18    2048      3.339    -6.188
   19    2819      3.479    -6.313
   20    3887      3.627    -6.442
   21    5402      3.762    -6.570
   22    7507      3.875    -6.697


SPACE DISTRIBUTION PROPERTIES

 Min. Fluence  1.00E-06  Total =  1331, Avg =  443.7 +/-  21.1
          1264 ( 94.97)        56 (  4.21)        11 (  0.83)

   DIPOLE: 0.065  at l=    0.90 and b =   0.13
   QUADRUPOLE:  eta= 0.053    zeta= 0.162

 Min. Fluence  1.00E-05  Total =  119, Avg =  39.7 +/-  6.3
            72 ( 60.50)        36 ( 30.25)        11 (  9.24)

   DIPOLE: 0.001  at l=  142.03 and b = -22.85
   QUADRUPOLE:  eta= 0.004    zeta= 0.008

 Min. Fluence  1.00E-04  Total =  8, Avg =  2.7 +/-  1.7
             2 ( 25.00)         3 ( 37.50)         3 ( 37.50)

   DIPOLE: 0.000  at l=  -16.53 and b = -38.89
   QUADRUPOLE:  eta= 0.000    zeta= 0.001

 Min. Fluence  1.00E-05  Total =  50, Avg =  16.7 +/-  4.1
            23 ( 46.00)        16 ( 32.00)        11 ( 22.00)

   DIPOLE: 0.002  at l=  173.18 and b = -16.47
   QUADRUPOLE:  eta= 0.001    zeta= 0.002
```

Figure 5. Sample output of monte carlo data analysis for the data set plotted in the previous figure. In addition to summarizing the parameters used to generate the model, the output lists the latitude distribution of the sample, the dipole moment, and parameters η and ζ of the quadrupole moment for a variety of minimum fluences. The angular anisotropies present at low minimum fluence disappear when considering only bright sources.

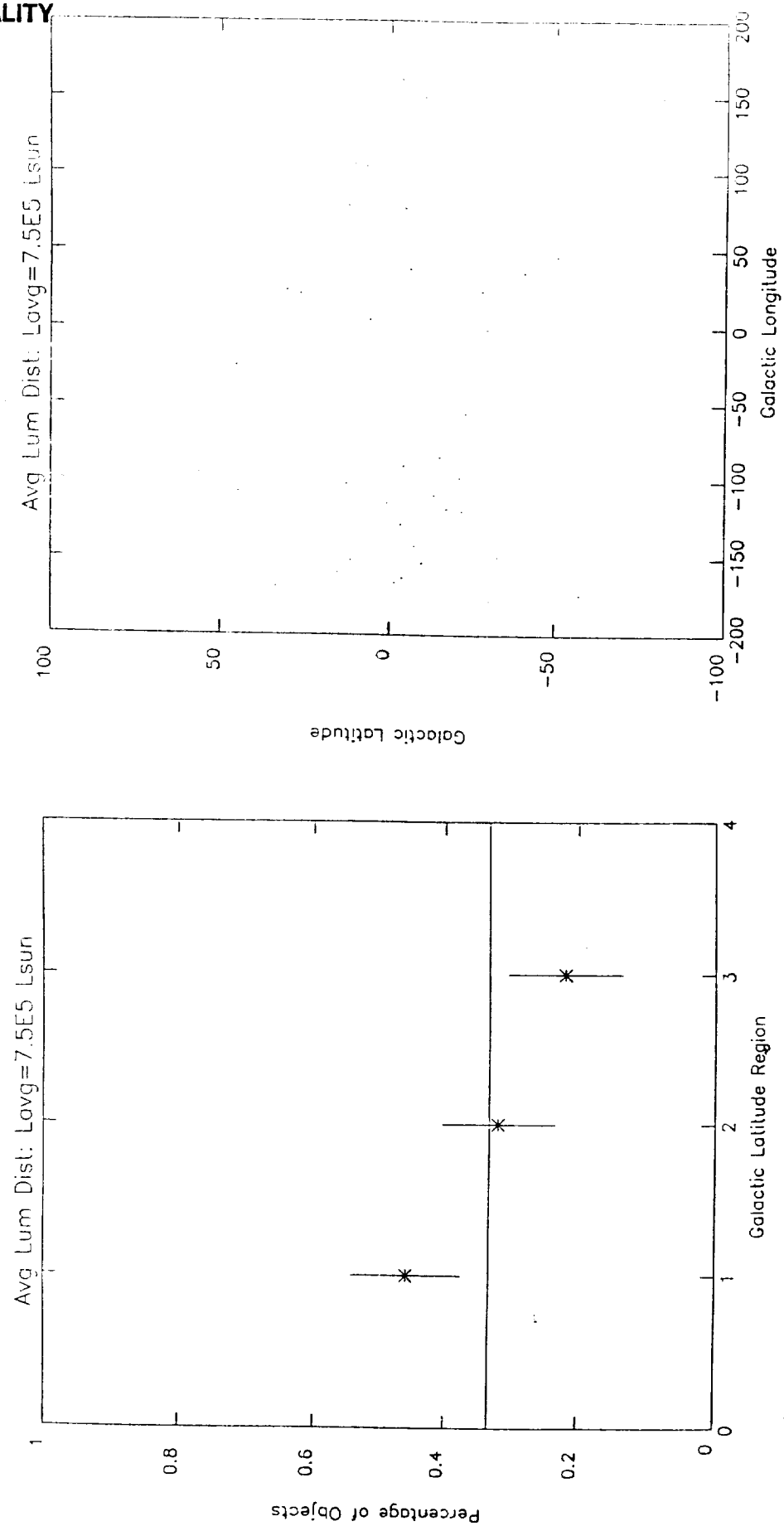

(a) (b)

Figure 6. Angular distribution plots for the sample described in the previous figures. The latitude distribution (a) and the local spatial distribution (b) are plotted for a minimum fluence of 2×10^{-5} erg cm^{-2}. Above this fluence, the sample is fairly isotropic.